Electron and positron contributions to the displacement per atom profile in bulk multi-walled carbon nanotube material irradiated with gamma rays

Antonio Leyva Fabelo, Ibrahin Piñera Hernández, Diana Leyva Pernía, Yamiel Abreu Alfonso y Carlos M. Cruz Inclán
Centro de Aplicaciones Tecnológicas y Desarrollo Nuclear (CEADEN) /
Calle 30 nº 502 entre 5ta y 7ma, Miramar, Playa, La Habana, Cuba
aleyva@ceaden.edu.cu

Abstract
The electron and positron contributions to the effective atom displacement cross-section in multi-walled carbon nanotube bulk materials exposed to gamma rays were calculated. The physical properties and the displacement threshold energy value reported in literature for this material were taken into account. Then, using the mathematical simulation of photon and particle transport in matter, the electron and positron energy flux distributions within the irradiated object were also calculated. Finally, considering both results, the atom displacement damage profiles inside the analyzed bulk carbon nanotube material were determined. The individual contribution from each type of secondary particles generated by the photon interactions was specified. An increasing behavior of the displacement cross-sections for all the studied particles energy range was observed. The particles minimum kinetic energy values that make probabilistically possible the single and multiple atom displacement processes were determined. The positrons contribution importance to the total number of point defects generated during the interaction of gamma rays with the studied materials was confirmed.

Key words: *carbon nanotubes, gamma radiation, atomic displacements, cross section, Monte Carlo method, simulation*

Aporte de electrones y positrones al perfil de desplazamientos atómicos en materiales masivos de nanotubos de carbono de paredes múltiples irradiados con rayos gamma

Resumen
Se presentan los resultados del cálculo de las contribuciones de los electrones y los positrones a la sección eficaz de desplazamiento de los átomos de carbono en materiales masivos constituidos por nanotubos de paredes múltiples. Para ello se tuvieron en consideración las propiedades físicas y la energía umbral de desplazamiento del carbono, reportadas en la literatura para este material. Se calculó también la distribución espacial de los flujos energéticos de los electrones y positrones dentro del blanco irradiado, utilizando la simulación matemática del transporte de los fotones y las partículas en la materia. Considerando ambos resultados, se determinaron los perfiles de daño por desplazamientos atómicos dentro del material masivo analizado, particularizando el aporte de cada tipo de partícula secundaria generada por la interacción de los fotones. Los resultados mostraron el comportamiento creciente de las secciones eficaces de desplazamiento en todo el intervalo de energía cinética evaluado. Se determinaron los valores de energías cinéticas de electrones y positrones a partir de los cuales son probabilísticamente posibles los procesos de desplazamientos atómicos simples y múltiples. Se confirmó la importancia del aporte de los positrones al número total de defectos puntuales generados durante la interacción de los rayos gamma con el material estudiado.

Palabras clave: *nanotubos de carbono, radiación gamma, desplazamientos atómicos, sección eficaz, método de Monte Carlo, simulación*

Introduction

The irradiation techniques are an effective method for the controlled generation of defects in carbon nanostructured materials. They are used in order to modify its properties, or to facilitate some processes such as coalescence, functionalization, formation of tunneling barriers, couplings creation and some others [1-5]. It is well known that the formation of radiation-induced defects in carbon nanostructures change their mechanical and electronic properties and may even cause catastrophic structural alterations [6, 7]. In this sense, understanding the formation of radiation-induced defects in these materials and its quantification is essential for the so-called defect-assisted engineering of nanomaterials [8]. These studies are also very important for the development of other applications related to nuclear, aerospace and medical technologies, where devices and materials based on carbon nanostructures are habitually exposed to aggressive radiation environments. Examples of these applications could be radiation detectors, solar cells, batteries, electronic microcircuits, etc. [9-12]. The thorough knowledge of the radiation response of these materials and devices, its radiation resistance and the dose thresholds is decisive for modern and future science and technology.

For the present study, gamma rays have been selected as radiation source due to their high penetration capability and their ability to generate stable point defects through the emitted secondary particles [7, 13, 14]. Gamma rays are often present in any nuclear facility, either for research, energy generation or medical therapy purposes. Moreover, in outer space this radiation forms part of an energetic and dense radiation background.

Although the study of gamma rays effects on different carbon nanostructures is reported in scientific literature, see for example [2, 7, 15], the influence of gamma radiation on defects generation in bulk multi-walled carbon nanotubes (B-MWCNT) materials is investigated for the first time. In particular, the carbon atom displacement cross-section (σ_{dpa}) for electrons and positrons had not been reported. Neither the sample in-depth distribution of the generated displacements per atom total number (N_{dpa}) nor its electron and positron contributions had been studied.

Knowledge of these data and facts provides new evidences to the understanding of the gamma radiation damage phenomenon in advanced materials, such as B-MWCNT, which is essential for safe and reliable exploitation and generalization of its applications.

Materials and Methods

The studied samples consist of B-MWCNT with mass densities of 1.36 g cm^{-3} and 1.45 g cm^{-3}, which correspond to 24.4% and 19.4% porosities respectively. These values were experimentally measured in B-MWCNT samples fabricated by spark plasma sintering [16].

The effective atom displacement cross-sections were calculated using the MCCM (Monte Carlo assisted Classical Method) algorithm. This software takes into account the McKinley-Feshbach approach [17] with the Kinchin-Pease approximation [18] for the damage function. A more complete and detailed explanation of this procedure can be found in [19].

Figure 1 shows a graphical representation of the simulated experiment. A multi-walled carbon nanotubes cylindrical shaped sample (100 μm diameter and 10 μm thickness) is irradiated with monochromatic photons of given energies. These photons impact perpendicularly and homogeneously distributed over the top surface of the cylinder. The atom displacement profile determination is performed in a 10 μm x 10 μm x 10 μm voxel located in the center of the cylinder.

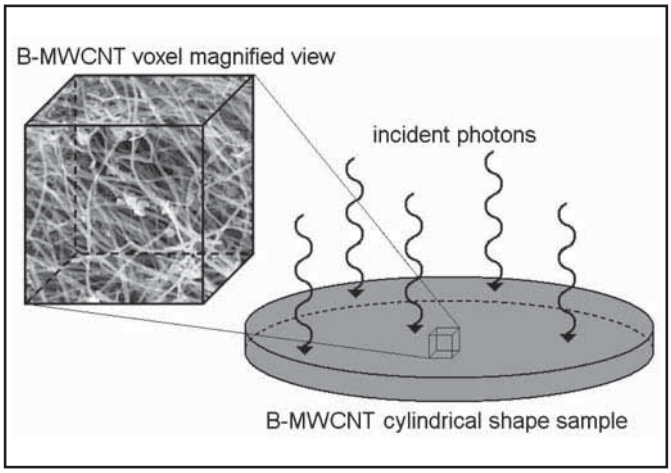

Figure 1. Graphical representation of the gamma irradiated B-MWCNT sample

The energy fluxes of electrons and positrons were calculated at different depths within the selected voxel. This calculation was accomplished with the use of MCNPX (Monte Carlos n - Particles Transport Code) software [20], which simulates the transport of photons and particles in matter. The obtained energy fluxes results were processed by the MCCM program to determine the number of atom displacements with depth in the selected voxel for each kind of secondary particle.

All simulation results are reported with a relative statistical error lower than 1%, which was ensured using a large number (10 million) of simulated incident photons and its secondary particles.

The displacement threshold energy, E_d, is an important characteristic describing the radiation hardness of the material. It is related not only to the bond energy but also to the local chemical bonding, to the availability of open space in the structure, and it may depend on the system geometry (e.g. diameter of a nanotube, incidence angle of radiation). Due to this, the determination of E_d is complicated, and for our target material a wide range of Ed values are reported in the literature. This threshold energy interval is usually between 15 and 20 eV [21, 22]. For this work was selected the average value E_d = 19.3 eV reported in [23], where the authors studied the angular dependence

of the threshold energy using molecular-dynamics simulations.

Results and Discussion

Gamma radiation is not able to directly transfer the energy needed to produce atom displacements, therefore the products of its interaction with matter (electrons and positrons) are responsible for this process. If the kinetic energy transferred from particle to the nucleus is higher than E_d, a carbon atom can leave its initial position to form a metastable structural defect on a subpicosecond time scale. The probability of this atom displacement process is determined by the displacement cross section, calculated using the previously explained methodology. Displacement cross section dependences with the secondary electron and positron kinetic energies (Ke_-, Ke_+) are shown in Figure 2. The behaviors of these two plots are similar, increasing with energy within the entire studied energy interval. Values of σ_{dpa} calculated for electrons are lightly higher than those of positrons, but no more than 3.36% in average.

As can be accurately observed in the inset graph of Figure 2 (magnification of the low energy region, $K_{e-,e+} \leq 1$ MeV), atom displacements processes are energetically possible for particle energy ≥ 100 keV.

If the primary rejected atom has enough energy to displace another atom by atom-atom collisions, then multiple atoms displacements may take place. The multilayer structure and the bulk character of the studied sample increases the probabilities of occurring cascades processes. The precise moment when the multiple atoms displacements processes begin is observable in Figure 2 at the point where an abrupt curves slope change takes place. As seen, the energy at which the atom displacement cascades begin is ~ 500 keV for both, electrons and positrons.

Figure 3 shows the calculation results for the total number of displacements per atom as a function of the incident photon energy for two mass density values. Here, N_{dpa} denotes the sum of all the involved particles contributions to dpa in the whole voxel volume. In this figure it is observed that N_{dpa} behaviors with photon energy are monotonous increasing in the whole studied energy range. For photon energies higher than 20 MeV, difference between the two distributions is almost constant, being approximately 6% superior for the sample with ρ = 1.45 g cm^{-3}.

The behaviors of the total number of atom displacements with depth inside the sample for both analyzed mass densities are presented in Figure 4. Here, reported Ndpa values refer to the total number of stable defects

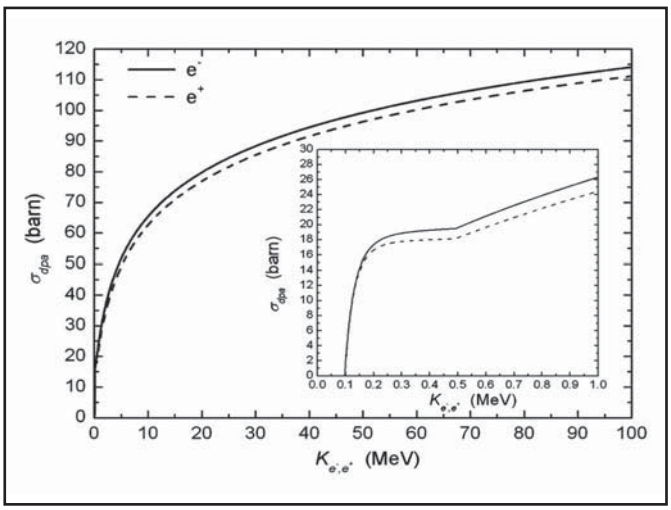

Figure 2. Displacement cross section behaviors with the electron and positron kinetic energies

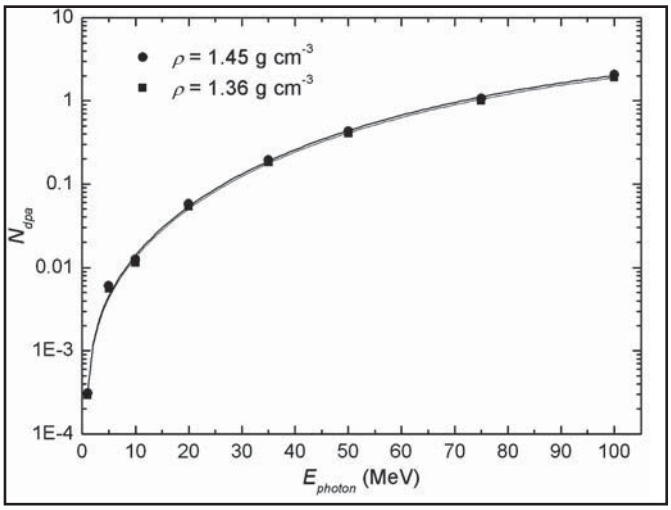

Figure 3. N_{dpa} behavior with the photon energy for two B-MWCNT mass densities. The lines are visual guides

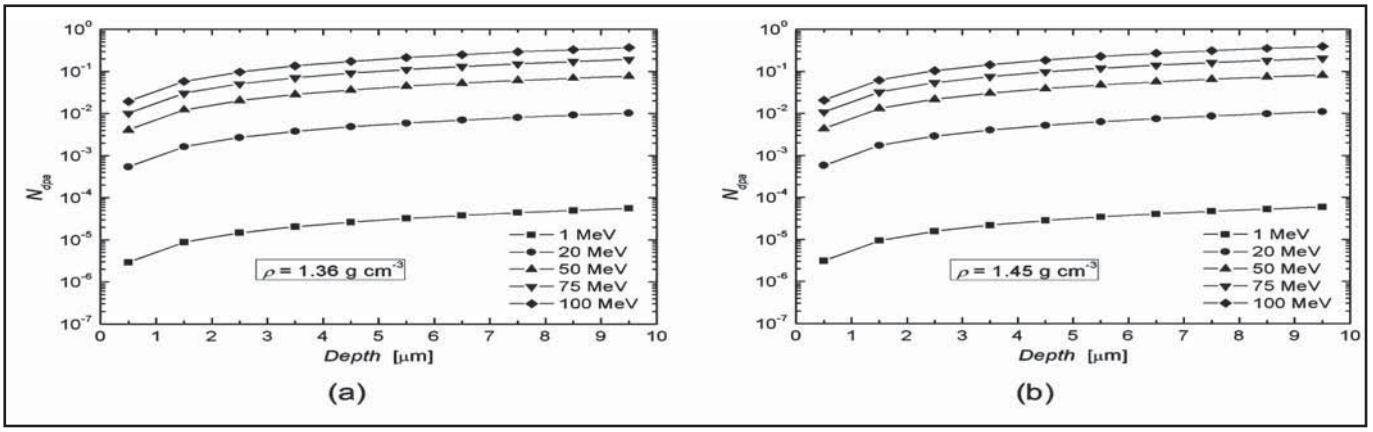

Figure 4. N_{dpa} in depth profiles in analyzed B-MWCNT sample for five photon energies and mass densities 1.36 g cm-3 (a) and 1.45 g cm-3 (b). The lines are visual guides

generated in a 1 μm thick layer within the voxel shown in Figure 1. These layers are located parallel at different depths in a continuous arrangement and perpendicularly to the incident photons direction.

For both analyzed sample mass densities, the N_{dpa} in-depth dependences increase monotonically along the entire sample, thus showing inhomogeneous volume distribution within the sample for all studied energies. The N_{dpa} highest values are located near to the sample surface opposite to the incidence surface.

Taken as reference the N_{dpa} values generated by the low-energy photons (1 MeV), the number of point defects produced by the other examined energies (20, 50, 75 and 100 MeV) were found to be higher by about 180, 1400, 3500 and 6600 times respectively, regardless of the depth where the events take place and the mass density of the studied samples.

At first sight the differences between the profiles presented in Figure 4 (a) and (b) are not observable. Detailed analysis showed that the distributions corresponding to the higher mass density sample were on average 6.59% higher than those ones belonging to the lighter sample. This small difference between the defects numbers created in the sample volume is closely related to the ratio between the two mass densities (6.62%). This result is reasonable because the density parameter appears as a linear factor in the used formalism for calculating the dpa and it is the one parameter that changes in the simulated experiment.

Figure 5 (a) and (b) present the results of the N_{dpa} decomposition in its two components, the electron and the positron contributions. The first conclusion from the analysis of these two figures is that the relationship between N_{dpa} partial contributions dependence to the mass density is negligible.

As it is observed in both figures, at low energies the positrons contribution to the stable structural point defects formation is significantly lower than the electrons one. For photons energies lower than 1.02 MeV positrons contribution is completely absent, as expected.

With increasing photon energy the occurrence probability of the pair formation phenomenon growths, generating a larger number of positrons and increasing their maximum kinetic energies. The positron displacement cross section (see Figure 2) and the particle range also rise with the particle energy.

All this leads to the observed behaviors in Figure 5 (a) and (b); with increasing photon energy, the weight of the positron component grows up to close to the electronic component. The positrons contribution to the total number of dpa generated in the sample were found to be 3.8%, 11.4%, 35.5% and 41.8% for photon energies of 5, 10, 50 and 100 MeV respectively.

As it can be seen, positrons contribute substantially to the total number of atom displacements in the analyzed structure exposed to radiation. This fact contradicts the assertion made by some authors whom claim that, since the generated positron subsequently annihilates by combining with an electron, its effect on atom displacement is negligibly small, and they are not included it in the calculation. For example, in [24] the authors present the results in the determination of the displacement cross section in various materials including C for gamma energies up to 14 MeV, avoiding in all cases the positron contributions to the displacement damage. Following the used methodology, we have determined that for 14 MeV gamma energy the positron contribution to the total displacement number in B-MWCNT sample (carbon allotrope) is about 16%, value which cannot be considered negligible. In previous studies, where bulk fullerene C60 [25] and YBCO superconducting materials [26] where studied following the same procedure as here, similar results were obtained. In summary, these results prove that the positron contribution cannot be ignored, and it takes a significant importance when increasing photon energy.

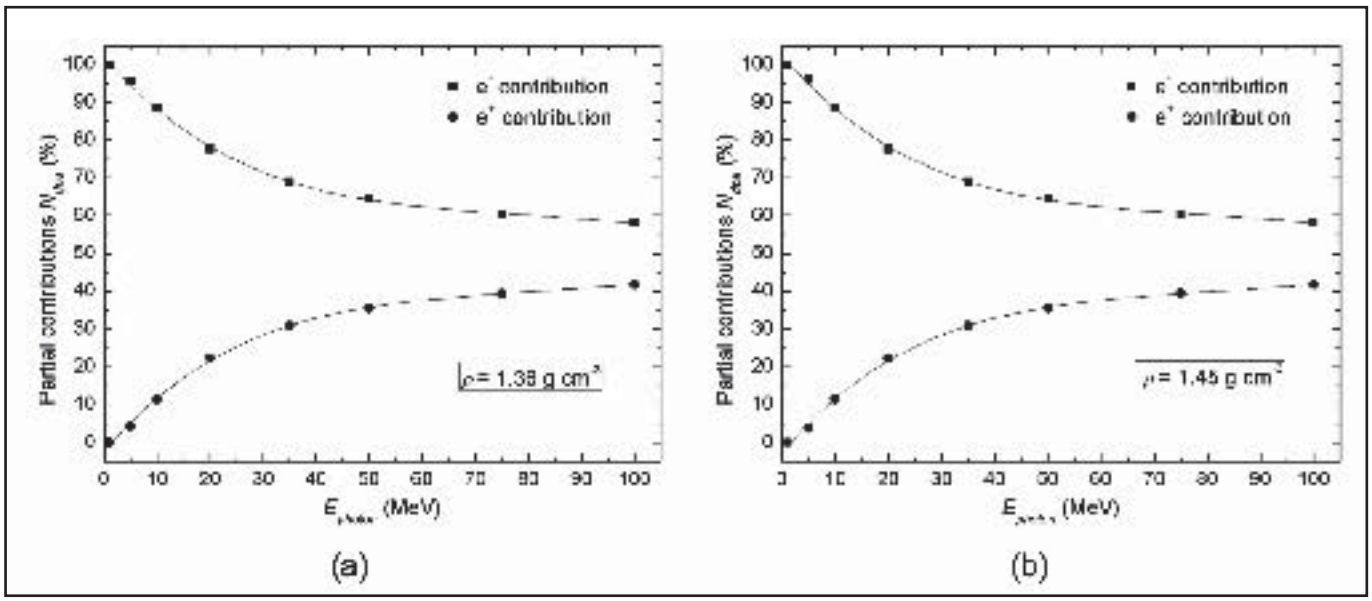

Figure 5. Behavior of the electron and positron contributions to the N_{dpa} with the photon energy for B-MWCNT mass densities 1.36 g cm^{-3} (a) and 1.45 g cm^{-3} (b). The lines are visual guides

Conclusions

The atom displacement cross section dependences with the secondary electron and positron kinetic energies for B-MWCNT were calculated in the energy range up to 100 MeV. Both behaviors are increasing with the energy and the values obtained for electrons are on average 3.36% higher than for positrons. The displacements processes start at particle energy ~ 100 keV and the multiple atoms displacements begin at energy close to 500 keV for both electrons and positrons. The total number of displacements per atom as a function of the incident photon energy was determined for two mass densities. These profiles show a monotonous increasing behavior in all the energy range, with values which are 6.6% higher for the sample with greater mass density. The dependence with depth of the total number of atom displacements is also monotonically increasing along the entire sample, with slopes growing up with photon energy. The electron and positron contributions to the N_{dpa} as a function of photon energy were presented, showing that the relationship between N_{dpa} partial contributions dependence to mass density is negligible. At very low energies the positrons contribution to the N_{dpa} is small, but its role increases with photon energy, reaching the 3.8%, 11.4%, 35.5% and 41.8% for photon energy of 5, 10, 50 and 100 MeV respectively. This behavior is independent of the B-MWCNT target mass density. These results confirm once again that the positron contribution to the atom displacements in materials should be considered, taking more importance when increasing the incident photon energy.

Acknowledgements

This work was supported by the AENTA of Cuba through the project PRN/6-2/3.

References

[1] ISMAT S, HASSNAIN G, YASSITEPE E, ALI B. Evaporation: processes, bulk microstructures, and mechanical properties. Chapter 4. In: Handbook of deposition technologies for films and coatings: science, applications and technology. Third Edition. Elsevier Inc., 2010. p. 135-252.

[2] SKAKALOVA V, DETTLAFF-WEGLIKOWSKA U, ROTH S. Gamma-irradiated and functionalized single wall nanotubes. Diamond and Related Materials. 2004; 13(2): 296-298.

[3] DMYTRENKO OP, KULISH NP, BELYI NM, et al. Dose dependences of the optical properties of fullerene films subjected to the electron irradiation. Thin Solid Films. 2006; 495(1-2): 365-367.

[4] DHARAMVIR K, JEET K, DU C, et al. Structural Modifications of Multiwalled Carbon Nanotubes by Swift Heavy Ions Irradiation. Journal of Nano Research. 2010; 10: 1-9.

[5] RODRÍGUEZ JA, TOLVANEN A, KRASHENINNIKOV AV, et al. Defect-induced junctions between single- or double-wall carbon nanotubes and metal crystals. Nanoscale. 2010; 2(6): 901-905.

[6] KRASHENINNIKOV AV, NORDLUND K. Ion and electron irradiation-induced effects in nanostructured materials. J. Appl. Phys. 2010; 107(7): 071301-071370.

[7] ZHIWEI X, LEI C, LIANGSEN L, et. al. Structural changes in multi-walled carbon nanotubes caused by gamma-ray irradiation. Carbon. 2011; 4(1): 350-351.

[8] YAZYEV OV, TAVERNELLI I, ROTHLISBERGER U, HELM L. Early stages of radiation damage in graphite and carbon nanostructures: A first-principles molecular dynamics study. Phys. Rev. B. 2007; 75(11): 115418-115422.

[9] THEOCHAROUS SP, THEOCHAROUS E, LEHMAN JH. The evaluation of the performance of two pyroelectric detectors with vertically aligned multi-walled carbon nanotube coatings. Infrared Physics & Technology. 2012; 55(4): 299–305.

[10] PINGFAN D, LIXIN S, JIE X, et al. Dye-sensitized solar cells based on anatase TiO2/multi-walled carbon nanotubes composite nanofibers photoanode. Electrochimica Acta. 2013; 87(1): 651-656.

[11] ZHILI X, YOUNG SY, HYOUNG-JOON J. Applications of Carbon Nanotubes for Lithium Ion Battery Anodes. Materials. 2013; 6(3): 1138-1158.

[12] JOO-HYUNG K, SUNGRYUL Y, HYUN-U K, JAEHWAN K. A flexible paper transistor made with aligned single-walled carbon nanotube bonded cellulose composite. Current Applied Physics. 2013; 13(5): 897-901.

[13] JOVANOVIC SP, MARKOVIC ZM, KLEUT DN, et al. A novel method for the functionalization of gamma-irradiated single wall carbon nanotubes with DNA. Nanotechnology. 2009; 20(44): 4456021-4456028.

[14] VITUSEVICH SA, SYDORUK VA, PETRYCHUK MV, et al. Transport properties of single-walled carbon nanotube transistors after gamma radiation treatment. J. Appl. Phys. 2010; 107(6): 063701-063707.

[15] LEE KY, KIM KY. 60Co gamma-ray irradiation effect and degradation behaviors of a carbon nanotube and poly(ethylene-co-vinyl acetate) nanocomposites. Polymer Degradation and Stability. 2008; 93(7): 1290-1299.

[16] ZHANG HL, LI JF, YAO KF, CHEN LD. Spark plasma sintering and thermal conductivity of carbon nanotube bulk materials. J. Appl. Phys. 2005; 97(11): 114310-114315.

[17] MCKINLEY WA, FESHBACH H. The coulomb scattering of relativistic electrons by nuclei. Phys. Rev. 1948; 74(12): 1759-1763.

[18] KINCHIN GH, PEASE RS. The displacement of atoms in solids by radiation. Rep. Prog. Phys. 1955; 18(1): 1-51.

[19] PIÑERA I, CRUZ C, ABREU Y, et. al. Monte Carlo assisted classical method for the calculation of dpa distribution in solid materials. IEEE Nuclear Science Symposium Conference Record, 2008. NSS '08. IEEE. Dresden, Germany. 19-25 Oct. 2008. p. 2557-2560. doi: 10.1109/NSSMIC.2008.4774878.

[20] HENDRICKS JS, MCKINNEY GW, TRELLUE HR, et. al. MCNPXTM (version 2.6.B). Report LA-UR-06-3248. Los Alamos National Laboratory, 2006.

[21] BANHART F. Irradiation effects in carbon nanostructures. Rep. Prog. Phys. 1999; 62(8): 1181-1221.

[22] BANHART F, FULLER T, REDLICH Ph, AJAYAN PM. The formation, annealing and self-compression of carbon onions under electron irradiation. Chem. Phys. Lett. 1997; 269(3-4): 349-355.

[23] CUI FZ, CHEN ZJ, MA J, et al. Atomistic simulation of radiation damage to carbon nanotube. Physics Letters A. 2002; 295(1): 55-59.

[24] KWON J, MOTTA AT. Gamma displacement cross-sections in various materials. Annals of Nuclear Energy. 2000; 27(18): 1627-1642.

[25] LEYVA A, PIÑERA I, LEYVA D, et. al. Monte Carlo calculation of carbon atom displacement damage in C60 fullerene bulk materials irradiated with gamma rays. Nucleus. 2012; (51): 20-25.

[26] PIÑERA I, CRUZ C, ABREU Y, et. al. Monte Carlo simulation study of positron contribution to displacement per atom production in YBCO superconductors. Nucl. Inst. Meth. Phys. Res. Section B. 2008; 266(22): 4899-4902.

Recibido: 10 de diciembre de 2012
Aceptado: 25 de abril de 2013